

Receding Horizon Iterative Learning Control for Continuously Operated Systems

Maxwell Wu¹, Mitchell Cobb², James Reed³, Kirti Mishra⁴, Chris Vermillion⁵, and Kira Barton⁶

Abstract—This paper presents an iterative learning control (ILC) scheme for continuously operated repetitive systems for which no initial condition reset exists. To accomplish this, we develop a lifted system representation that accounts for the effect of the initial conditions on dynamics and projects the dynamics over multiple future iterations. Additionally, we develop an economic cost function and update law that considers the performance over multiple iterations in the future, thus allowing for the prediction horizon to be larger than just the next iteration. Convergence of the iteration varying initial condition and applied input are proven and demonstrated using a simulated servo-positioning system test case.

I. INTRODUCTION

FOR systems that exhibit repetitive behavior, repetitive and iterative learning control (ILC) techniques have proven to be useful tools that enable system performance to be improved through a learning-based update of the control signal. Traditionally, these strategies have aimed to eliminate tracking error of a known reference signal by leveraging information available in previous executions of a task to counteract uncertainties in the system. Typically, ILC has been developed for batch processes wherein the system undergoes an initial condition reset between iterations of the repetitive task. A common method of implementation of ILC controllers is depicted in the block diagram shown in Figure 1. Here, measurements of the system states and outputs, as well as knowledge of previously applied control signals, initial conditions, and reference signals, are utilized to design improved control signals in future iterations [1]. Meanwhile, repetitive control has generally been used for continuous processes where no such reset of the initial condition occurs between iterations [2].

Many repetitive systems operate continuously. For instance, in autonomous racing applications the vehicle must repeatedly follow a predefined path with the goal of minimizing total lap time. Here, the control actions at a given lap will influence the behavior of the vehicle in future laps. Specifically, the system

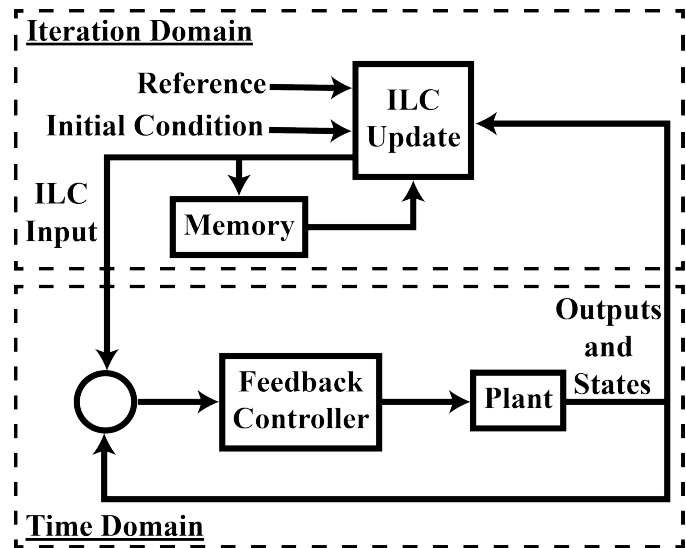


Figure 1: ILC utilizes iteration domain feedback to inform how a system is to be controlled in future iterations. An iteration-varying feedforward input signal aims to improve the behavior of the system by compensating for model uncertainties.

is considered continuously operable in that the initial condition at each iteration is given by the terminal condition at the previous iteration. Additionally, note that here the performance is not strictly dependent on the ability of the system to accurately track a predefined reference trajectory. Rather, the improved performance is achieved if the system is better able to minimize the non-traditional performance metric of lap time. These *economic* metrics enable system performance to be assessed for a broader range of systems such as robotic prosthetic legs that aim to follow a continuous gait trajectory while expending as little energy as possible, or tethered energy systems that follow a repetitive closed flight path with the primary objective of maximizing power generation.

Traditionally, repetitive control design has relied on a frequency domain analysis wherein the internal model principle is employed for the purpose of tracking periodic references or rejection of periodic disturbances [2]. However, while suitable for strict trajectory tracking objectives, controller design in the frequency domain is difficult to exercise when improvement in more general economic performance metrics is desired. On the other hand, ILC design has often leveraged state space models to improve system performance through iteration-based feedback. The use of state-space analysis has enabled the development of system representations in the lifted

¹Maxwell Wu is a PhD candidate at The University of Michigan maxwu@umich.edu.

²Mitchell Cobb is a controls engineer at Blue Origin mcobb@ncsu.edu.

³James Reed is an a PhD candidate at North Carolina State University jcreed2@ncsu.edu.

⁴Kirti Mishra is a Postdoctoral researcher at North Carolina State University kdmishra@ncsu.edu.

⁵Chris Vermillion is an Associate Professor in the Department of Mechanical and Aerospace Engineering at North Carolina State University, Raleigh, NC 27695, USA cvermil@ncsu.edu.

⁶Kira Barton is an Associate Professor in the Department of Mechanical Engineering at the University of Michigan, Ann Arbor, MI, 48109, USA bartonkl@umich.edu.

domain, as well as ‘norm-optimal’ controller design, which permits the intuitive construction of quadratic cost functions as a function of the control signal [3].

Historically, ILC designs have been made to minimize these cost functions by updating the feedforward control signal from data obtained in the previous iteration. While such strategies have proven useful, by only using information from a single iteration, these techniques neglect potential benefits to system performance that can be obtained by utilizing information from multiple iterations. To combat this, a subfield of ILC called ‘predictive iterative learning control’, as described in [4], [5], [6], [7], and [8], has been developed that not only uses information from the previous iteration, but also uses predictions of system behavior in future iterations to update the control signal. These strategies have shown improved convergence rates in comparison to traditional ILC while still establishing requirements for stability. However, these works consider a class of systems where the initial condition is reset between iterations.

To accommodate continuously operable systems, several techniques have been created. The strategy given by [9] and [10] iteratively updates safe sets over which system constraints are satisfied. A model predictive control optimization problem is then solved where the enlarged safe sets allow for a broader selection of control signals to be applied, thus giving opportunities for improved performance. This strategy has been previously used for the autonomous racing application described above and shown to be effective in reducing total lap time. However, this formulation dispenses with the ‘lifted system’ representation commonly used in ILC, as well as learning filters used to construct a closed form update law. In [11] and [12], a state-space based repetitive control strategy is designed to minimize performance of a system over an infinite prediction horizon by describing the problem as an iteration-domain LQ regulation problem with a control law given by solution of the algebraic Riccati equation. However, only the infinite horizon case is considered and no analysis giving requirements for stability or robustness to disturbances is given.

To address these issues, a receding horizon ILC formulation is developed for application to continuously operated systems. The contributions of this paper are given by

- 1) Generation of a lifted system representation that describes the impact of initial conditions and a multi-iteration control signal on the system dynamics.
- 2) A closed form update law that describes how the control signal is updated to reduce the value of a multi-iteration cost function.
- 3) An analysis of conditions for closed loop stability and desired system performance with considerations toward robustness to uncertain plant dynamics and disturbances.
- 4) Implementation of the algorithm to linear time-invariant and linear time varying systems.

II. RECEDING HORIZON ITERATIVE LEARNING CONTROL

The proposed ILC formulation contains two features that facilitate the consideration of continuous operation where an

initial condition reset between cycles does not exist. This is achieved by combining a lifted system model that explicitly includes the impact of nonzero initial conditions with a performance index that includes predicted performance over multiple future iterations. Thus, the framework is capable of implicitly considering the impact of control decisions from one iteration on future iterations. The resulting iterative update law then provides control sequences for multiple future iterations. However, due to the need to adjust for disturbances and modeling uncertainties and inaccuracies, this feedforward control sequence is only applied one iteration at a time before being updated. The following subsections detail this approach.

A. Multi-Iteration System Model

We first consider systems with discrete time dynamic models of the form

$$x_j^{k+1} = \mathbf{A}x_j^k + \mathbf{B}u_j^k \quad (1)$$

with state vector $x \in \mathbb{R}^{n_x}$ and control input $u \in \mathbb{R}^{n_u}$ where $k \in \mathbb{N}$ is a timestep index, $j \in \mathbb{N}$ is an iteration index, and n_x and n_u indicate the number of states and inputs. We specifically consider the case where $n_u = 1$. \mathbf{A} and \mathbf{B} are appropriately sized, real valued matrices. We now define the lifted vectors

$$\begin{aligned} \underline{x}_j &\triangleq \left[(x_j^1)^T \quad (x_j^2)^T \quad \dots \quad (x_j^{n_s-1})^T \quad (x_j^{n_s})^T \right]^T \\ \underline{u}_j &\triangleq \left[(u_j^0)^T \quad (u_j^1)^T \quad \dots \quad (u_j^{n_s-2})^T \quad (u_j^{n_s-1})^T \right]^T, \end{aligned} \quad (2)$$

which give the state and input sequences over iteration j . Using this notation gives the lifted system model

$$\underline{x}_j = \underline{\mathbf{G}}\underline{u}_j + \underline{\mathbf{F}}x_j^0 \quad (3)$$

where x_j^0 denotes the initial condition at iteration j and $\underline{\mathbf{G}} \in \mathbb{R}^{n_s n_x \times n_s}$ is a block matrix where the block element $\underline{\mathbf{G}}_{m,p} \in \mathbb{R}^{n_x}$ in the m^{th} block row and p^{th} column of $\underline{\mathbf{G}}$ is given by

$$\underline{\mathbf{G}}_{m,p} = \begin{cases} \mathbf{0}^{n_x} & m < p \\ \mathbf{A}^{m-p} \mathbf{B} & m \geq p. \end{cases} \quad (4)$$

Similarly, the block element in the m^{th} block row of $\underline{\mathbf{F}} \in \mathbb{R}^{n_s n_x \times n_x}$ is given by

$$\underline{\mathbf{F}}_m = \mathbf{A}^m. \quad (5)$$

As the system is considered to be operated continuously, the initial conditions are not reset between iterations. More specifically, the terminal condition from iteration j is equal to the initial condition at iteration $j + 1$. Consequently, with a shift in the iteration index, (3) can be alternatively expressed as

$$x_{j+1} = \underline{\mathbf{G}}\underline{u}_{j+1} + \underline{\mathbf{F}}\mathbf{E}_F x_j \quad (6)$$

where

$$\mathbf{E}_F \triangleq \left[\mathbf{0}^{n_x \times n_x(n_s-1)} \quad \mathbb{I}^{n_x \times n_x} \right], \quad (7)$$

which is used to select the terminal states from the \underline{x}_j vector.

For causal systems that lack an initial condition reset, the control sequence chosen for one iteration has a direct

Substituting (9) and (12) into (15), allows for \mathbf{J}_{j+n_i} to be expressed solely as a function of the known quantities \underline{u}_j , x_j^0 , and x_{j+1}^0 , as well as the design parameter \mathbf{u}_{j+1} .

We can obtain an expression for the performance index completely in terms of the known quantities from the last iteration, \underline{u}_j , and \underline{x}_j , along with the control sequences over the next several iterations, \mathbf{u}_{j+1} . Similar to the strategy employed in [13], by taking the gradient of \mathbf{J}_{j+1} with respect to \mathbf{u}_{j+1} , setting the result equal to the zero vector, and re-arranging the resulting expression, we obtain the update law

$$\mathbf{u}_{j+1} = \mathbf{L}_u \underline{u}_j + \mathbf{L}_e \underline{e}_j + \mathbf{L}_{x_j^0} x_j^0 + \mathbf{L}_{x_{j+1}^0} x_{j+1}^0 + \mathbf{L}_c \quad (18)$$

where

$$\begin{aligned} \mathbf{L}_0 &\triangleq \hat{\mathbf{Q}}_u + \mathbf{G}^T (\hat{\mathbf{Q}}_x + \hat{\mathbf{Q}}_e) \mathbf{G} \\ \mathbf{L}_u &\triangleq \mathbf{L}_0^{-1} (\mathbf{E}_u^T \mathbf{Q}_{\delta u} + \mathbf{G}^T \hat{\mathbf{Q}}_e \mathbf{I}_x \mathbf{G} + (\mathbf{E}_x \mathbf{G})^T \mathbf{Q}_{\delta x} \mathbf{G}) \\ \mathbf{L}_e &\triangleq \mathbf{L}_0^{-1} \mathbf{G}^T \hat{\mathbf{Q}}_e \mathbf{I}_x \\ \mathbf{L}_{x_j^0} &\triangleq \mathbf{L}_0^{-1} ((\mathbf{E}_x \mathbf{G})^T \mathbf{Q}_{\delta x} \mathbf{F} + \mathbf{G} \hat{\mathbf{Q}}_e \mathbf{I}_x \mathbf{F}) \\ \mathbf{L}_{x_{j+1}^0} &\triangleq -\mathbf{L}_0^{-1} \mathbf{G}^T (\hat{\mathbf{Q}}_x + \hat{\mathbf{Q}}_e) \mathbf{F} \\ \mathbf{L}_c &\triangleq -\mathbf{L}_0^{-1} \mathbf{G} \mathbf{s}_x \end{aligned} \quad (19)$$

and

$$\hat{\mathbf{Q}}_u \triangleq \mathbf{Q}_u + \mathbf{D}_u^T \mathbf{Q}_{\delta u} \mathbf{D}_u + \mathbf{E}_u^T \mathbf{Q}_{\delta u} \mathbf{E}_u \quad (20)$$

$$\hat{\mathbf{Q}}_x \triangleq \mathbf{Q}_x + \mathbf{D}_x^T \mathbf{Q}_{\delta x} \mathbf{D}_x + \mathbf{E}_x^T \mathbf{Q}_{\delta x} \mathbf{E}_x \quad (21)$$

$$\hat{\mathbf{Q}}_e \triangleq \mathbf{Q}_e. \quad (22)$$

Hence, as depicted in the block diagram in Figure 1, the ILC update utilizes information from the current input sequence, as well as the error signal and initial conditions to generate the feedforward input sequence at the next iteration.

Note that the update law given by (18) generates the super-lifted vector \mathbf{u}_{j+1} that describes the optimal control sequence to be applied over the next n_i iterations. While one approach might be to apply the control sequence given by \mathbf{u}_{j+1} over the next n_i iterations, an iteration-domain receding horizon approach is instead proposed where only the control sequence corresponding to the next iteration is applied before recomputing the optimal super-lifted control sequence. In other words, the control sequence given by

$$\underline{u}_{j+1} = \mathbf{E}_u \mathbf{u}_{j+1} \quad (23)$$

is applied over iteration $j+1$. This strategy mimics the control law used in generalized predictive control as described in [14], as well as model predictive control. By updating the control sequence after every iteration, we incorporate the most recent information, making the system more robust to disturbances and modeling uncertainties. We describe the resulting control structure as iteration-domain receding horizon control or receding horizon iterative learning control (RHILC).

III. CONTROLLER ANALYSIS

The stability properties and desired system behavior of the RHILC controller are now examined.

A. Stability Analysis

We consider the application of the RHILC algorithm to a plant with dynamics given as

$$x_j^{k+1} = \mathbf{A}_j x_j^k + \mathbf{B}_j u_j^k + d_j^k. \quad (24)$$

where \mathbf{A}_j and \mathbf{B}_j denote the iteration varying plant dynamics and $d_j \in \mathbb{R}^{n_x}$ is a disturbance. From (4) and (5), the plant dynamics can be expressed in lifted form as

$$\underline{x}_j = \underline{\mathbf{G}}_j \underline{u}_j + \underline{\mathbf{F}}_j x_j^0 + \underline{d}_j \quad (25)$$

where $\underline{\mathbf{G}}_j$ and $\underline{\mathbf{F}}_j$ are iteration varying plant matrices and $\underline{d}_j \in \mathbb{R}^{n_s n_x}$ captures the effect of the disturbance on the state sequence.

Since the system operates continuously such that $x_{j+1}^0 = \mathbf{E}_F \underline{x}_j$, substitution of (25) yields that the initial condition at each iteration evolves according to

$$x_{j+1}^0 = \mathbf{E}_F \left(\underline{\mathbf{G}}_j \underline{u}_j + \underline{\mathbf{F}}_j x_j^0 + \underline{d}_j \right). \quad (26)$$

Consequently, substituting (25) and (26) into (23) yields

$$\begin{aligned} \underline{u}_{j+1} = & \mathbf{T}_{u_j} \underline{u}_j + \mathbf{T}_{x_j^0} x_j^0 + \mathbf{E}_u \left(\mathbf{L}_e \underline{x} + (\mathbf{L}_{x_{j+1}^0} \mathbf{E}_F - \mathbf{L}_e) \underline{d}_j + \mathbf{L}_c \right) \end{aligned} \quad (27)$$

with

$$\mathbf{T}_{u_j} = \mathbf{E}_u \left(\mathbf{L}_u + \mathbf{L}_{x_{j+1}^0} \mathbf{E}_F \underline{\mathbf{G}}_j - \mathbf{L}_e \underline{\mathbf{G}}_j \right) \quad (28)$$

$$\mathbf{T}_{x_j^0} = \mathbf{E}_u \left(\mathbf{L}_{x_{j+1}^0} \mathbf{E}_F \underline{\mathbf{F}}_j + \mathbf{L}_{x_j^0} - \mathbf{L}_e \underline{\mathbf{F}}_j \right). \quad (29)$$

We then define the vector \underline{z}_j as

$$\underline{z}_j \triangleq \begin{bmatrix} \underline{u}_j \\ x_j^0 \end{bmatrix}, \quad (30)$$

which is the concatenation of the lifted input vector and initial condition at iteration j .

From (27) and (26), this then gives

$$\underline{z}_{j+1} = \mathbf{A}_{z_j} \underline{z}_j + \underline{\eta}_j \quad (31)$$

where

$$\mathbf{A}_{z_j} \triangleq \begin{bmatrix} \mathbf{T}_{u_j} & \mathbf{T}_{x_j^0} \\ \mathbf{E}_F \underline{\mathbf{G}}_j & \mathbf{E}_F \underline{\mathbf{F}}_j \end{bmatrix} \quad (32)$$

$$\underline{\eta}_j \triangleq \begin{bmatrix} \mathbf{E}_u (\mathbf{L}_e \underline{x} + (\mathbf{L}_{x_{j+1}^0} \mathbf{E}_F - \mathbf{L}_e) \underline{d}_j + \mathbf{L}_c) \\ \mathbf{E}_F \underline{d}_j \end{bmatrix}. \quad (33)$$

Hence, the evolution of the input sequence and initial condition can be described as a linear system.

The requirements for robust stability of the closed-loop system are now presented. Here, let $\rho(\Lambda)$ denote the spectral radius of square matrix Λ .

Condition 1. $\rho(\mathbf{A}_{z_j}) < 1$ for all j .

Condition 2. $\lim_{j \rightarrow \infty} \mathbf{A}_{z_j} = \mathbf{A}_z$ and $\lim_{j \rightarrow \infty} \underline{d}_j = \underline{d}$ for constants \mathbf{A}_{z_j} and \underline{d} .

Condition 1 is a general requirement for stability of linear systems. Condition 2 states that the dynamics of the plant, as well as the disturbance signal, converge over the iteration domain.

Corollary 1. *If Condition 1 holds, the system given by (31) is exponentially stable.*

Corollary 1 is obtained from standard linear systems theory. Additionally, the converged value of \underline{z}_j can be assessed.

Theorem 1. *If Conditions 1 and 2 hold, then*

$$\lim_{j \rightarrow \infty} \underline{z}_j = (\mathbf{I} - \mathbf{A}_z)^{-1} \underline{\eta} \text{ where } \underline{\eta} = \underline{\eta}_j(d) \quad (34)$$

Proof. Taking the limit of (31) gives

$$\lim_{j \rightarrow \infty} \underline{z}_{j+1} = \lim_{j \rightarrow \infty} (\mathbf{A}_z \underline{z}_j + \underline{\eta}_j) \quad (35)$$

Applying the assumptions on \mathbf{A}_{z_j} and \underline{d}_j gives

$$\lim_{j \rightarrow \infty} \underline{z}_{j+1} = \lim_{j \rightarrow \infty} \underline{z}_j = \lim_{j \rightarrow \infty} (\mathbf{A}_z \underline{z}_j + \underline{\eta}) \quad (36)$$

where

$$\underline{\eta} \triangleq \underline{\eta}_j(d),$$

which implies that

$$\lim_{j \rightarrow \infty} (\mathbf{I} - \mathbf{A}_z) \underline{z}_j = \underline{\eta}. \quad (37)$$

Thus,

$$\underline{z}_\infty \triangleq \lim_{j \rightarrow \infty} \underline{z}_j = (\mathbf{I} - \mathbf{A}_z)^{-1} \underline{\eta} \quad (38)$$

as a consequence of $\rho(\mathbf{A}_z) < 1$. \square

Hence, under satisfaction of Conditions 1 and 2, a closed form for the converged value of the input sequence and initial condition can be generated.

B. Desired Converged Controller Behavior

From Section III-A, requirements for robust convergence of the input sequence and initial condition are established. While meeting Conditions 1 and 2 establish sufficient criterion for convergence, note that the converged value of the input sequence and initial condition as given by \underline{z}_∞ is not necessarily the minimizer of \mathbf{J}_{j+n_i} . Hence, we now investigate what the input sequence and initial condition should be at convergence to achieve desired system behavior. For this, the operation matrices $\mathbf{E}_s \in \mathbb{R}^{n_s n_u (n_s n_u + n_x)}$ and $\mathbf{E}_e \in \mathbb{R}^{n_x (n_s n_u + n_x)}$ are introduced such that

$$\underline{u}_j = \mathbf{E}_s \underline{z}_j \quad (39)$$

$$\underline{x}_j^0 = \mathbf{E}_e \underline{z}_j. \quad (40)$$

are satisfied.

The optimization problem

$$\text{minimize}_{\underline{z}_{j+1}} \mathbf{J}_{j+n_i} \quad (41)$$

$$\text{subject to } \underline{u}_{j+1} = \mathbf{E}_s \underline{z}_{j+1} \quad (42)$$

$$\underline{x}_{j+1}^0 = \mathbf{E}_e \underline{z}_{j+1} \quad (43)$$

$$\underline{x}_{j+1} = \mathbf{G} \underline{u}_{j+1} + \mathbf{F} \underline{x}_{j+1}^0 + \underline{d} \quad (44)$$

$$\mathbf{e}_{j+1} = \bar{\mathbf{r}} - \mathbf{x}_{j+1} \quad (45)$$

$$\mathbf{u}_{j+1} = \mathbf{I}_u \underline{u}_{j+1} \quad (46)$$

$$\underline{u}_j = \underline{u}_{j+1} \quad (47)$$

$$\mathbf{x}_{j+1} = \mathbf{I}_x \underline{x}_{j+1} \quad (48)$$

$$\underline{x}_j = \underline{x}_{j+1} \quad (49)$$

$$\mathbf{E}_F \underline{x}_{j+1} = \underline{x}_{j+1}^0 \quad (50)$$

is now introduced. Here, (42) and (43) define how the input sequence and initial condition are given from the value of \underline{z} . Equation (44) defines the lifted state vector for the converged plant and disturbance while (45) gives the definition of the super-lifted error vector. Equations (46) and (47) constrain the input signal to have converged to a constant value while (48) and (49) constrain the state dynamics to have converged to a constant value. Constraint (50) requires that the terminal states must be equal to the initial condition from the beginning of the iteration.

To put constraints (46)-(49) into better context, note that the cost function is defined over a finite prediction horizon. Consequently, the minimizer of the cost function in the absence of these constraints may be greedy wherein low cost performance is given over the current prediction horizon, but the resulting initial condition at the iteration immediately following the prediction horizon may lead to poor future performance. Hence, the minimizer of the cost function without these constraints may not be desirable over many iterations. By adding these constraints, the solution of the optimization problem will give an input sequence and initial condition such that at convergence, applying the input sequence to the system with the optimal initial condition over a single iteration results in a state trajectory with a terminal condition equal to the initial condition. Thus, this combination of input sequence and initial condition is repeatable such that, at convergence, the same input sequence applied at every iteration will achieve the same performance. Consequently, note that in the optimization problem given by (41)-(50), the constraints imply that the value of the second, third, fifth, and sixth terms on the right hand side of (15) are equal to zero.

The problem given by (41)-(50) is an equality constrained optimization problem and can be expressed equivalently as

$$\text{minimize}_{\underline{z}_{j+1}} \frac{1}{2} \underline{z}_{j+1} \hat{\mathbf{Q}}_q \underline{z}_{j+1} + \hat{\mathbf{q}}_l^T \underline{z}_{j+1} \quad (51)$$

$$\text{subject to } \mathbf{W} \underline{z}_{j+1} = \mathbf{v}$$

where $\hat{\mathbf{Q}}_q, \hat{\mathbf{q}}_l, \mathbf{W}, \mathbf{v}$ are defined in Appendix VII-B.

Condition 3. *The matrix given by $\hat{\mathbf{Q}}_q + \mathbf{W}^T \mathbf{W}$ is positive definite.*

Theorem 2. Suppose that Condition 3 holds. Then the solution, \mathbf{z}_{opt} , of problem (51) can be found from

$$\begin{bmatrix} \mathbf{z}_{opt} \\ \lambda_{opt} \end{bmatrix} = \begin{bmatrix} \hat{\mathbf{Q}}_q & \mathbf{W}^T \\ \mathbf{W} & \mathbf{0} \end{bmatrix}^{-1} \begin{bmatrix} -\hat{\mathbf{q}}_l \\ \mathbf{v} \end{bmatrix}. \quad (52)$$

Proof. As (51) is an equality constrained quadratic program, the optimality condition

$$\begin{bmatrix} \hat{\mathbf{Q}}_q & \mathbf{W}^T \\ \mathbf{W} & \mathbf{0} \end{bmatrix} \begin{bmatrix} \mathbf{z}_{opt} \\ \lambda_{opt} \end{bmatrix} = \begin{bmatrix} -\hat{\mathbf{q}}_l \\ \mathbf{v} \end{bmatrix} \quad (53)$$

must hold where λ_{opt} denotes the vector of Lagrange multipliers. Condition 3 gives that the matrix on the left of the equation is non-singular, thus giving the desired result. \square

Therefore, satisfaction of Condition 3 yields a closed form for the optimal value of the input sequence and initial condition at convergence.

IV. STABILITY FOR LINEAR TIME-VARYING SYSTEMS

The RHILC control scheme described in Section II is developed using a system model given by (1) for application to plants with dynamics given by (24). Note, however, that the controller could also be developed for LTV system models of the form

$$\mathbf{x}_j^{k+1} = \mathbf{A}_j^k \mathbf{x}_j^k + \mathbf{B}_j^k \mathbf{u}_j^k \quad (54)$$

where \mathbf{A}_j^k and \mathbf{B}_j^k denote the time-varying state space matrices. In this case, (4) is rewritten as

$$\mathbf{G}_{m,p}^j = \begin{cases} \mathbf{0}^{n_x \times n_u} & m < p \\ \mathbf{B}_m^j & m = p \\ \mathbf{A}_j^m \mathbf{A}_j^{m-1} \dots \mathbf{A}_j^p \mathbf{B}_j^m & \text{otherwise.} \end{cases} \quad (55)$$

where j denotes the dependency on the iteration. Additionally, (5) is rewritten as

$$\mathbf{F}_m^j = \mathbf{A}_j^m \mathbf{A}_j^{m-1} \dots \mathbf{A}_j^2 \mathbf{A}_j^1. \quad (56)$$

which gives the lifted dynamics

$$\mathbf{x}_{j+1} = \mathbf{G}_{j+1} \mathbf{u}_{j+1} + \mathbf{F}_{j+1} \mathbf{E}_F \mathbf{x}_j. \quad (57)$$

The super-lifted dynamics

$$\mathbf{x}_{j+1} = \mathbf{G}_j \mathbf{u}_{j+1} + \mathbf{F}_j \mathbf{x}_j^0 \quad (58)$$

are then given by constructing \mathbf{G}_j as

$$\mathbf{G}_j \triangleq \begin{bmatrix} \mathbf{G}_j & \mathbf{0} & \dots & \dots & \mathbf{0} \\ \mathbf{F}_j \mathbf{E}_F \mathbf{G}_j & \mathbf{G}_j & \dots & \dots & \mathbf{0} \\ \vdots & \vdots & \ddots & \ddots & \vdots \\ \left(\prod_{m=1}^{N_i-1} \mathbf{F}_j \mathbf{E}_F \right) \mathbf{G}_j & \left(\prod_{m=1}^{N_i-2} \mathbf{F}_j \mathbf{E}_F \right) \mathbf{G}_j & \dots & \mathbf{G}_j & \mathbf{0} \\ \left(\prod_{m=1}^{N_i} \mathbf{F}_j \mathbf{E}_F \right) \mathbf{G}_j & \left(\prod_{m=1}^{N_i-1} \mathbf{F}_j \mathbf{E}_F \right) \mathbf{G}_j & \dots & \mathbf{F}_j \mathbf{E}_F \mathbf{G}_j & \mathbf{G}_j \end{bmatrix} \quad (59)$$

and \mathbf{F}_j as

$$\mathbf{F}_j \triangleq \begin{bmatrix} \mathbf{F}_j \\ \vdots \\ \left(\prod_{m=1}^{n_i-2} \mathbf{F}_j \mathbf{E}_F \right) \mathbf{F}_j \\ \left(\prod_{m=1}^{n_i-1} \mathbf{F}_j \mathbf{E}_F \right) \mathbf{F}_j \end{bmatrix}. \quad (60)$$

The learning filters are then defined using these updated super-lifted matrices \mathbf{G}_j and \mathbf{F}_j .

Satisfaction of Condition 1 then gives stability for the system given by (31) with \mathbf{A}_{z_j} and η_j given by the updated learning filters.

V. ILLUSTRATIVE EXAMPLE: SERVO-POSITIONING SYSTEM

The RHILC algorithm is now implemented in simulation to a servo-positioning system described in [15]. To demonstrate the advantages of using a receding horizon approach to continuously operating systems, simulations are conducted on an iteration-invariant nominal model using the strategy described in Section II-A. Additionally, simulations on an iteration varying model with added uncertainty are presented to demonstrate the effectiveness of the algorithm in a more practical case.

A. Simulation of Nominal System

Implementation of the RHILC algorithm is performed using varying prediction horizon lengths on a nominal model of the servo-positioning system with dynamics given as in [15] according to

$$\mathbf{A} = \begin{bmatrix} 0 & 1 \\ -0.71 & 1.50 \end{bmatrix}, \quad \mathbf{B} = \begin{bmatrix} 1 \\ 1 \end{bmatrix}. \quad (61)$$

Here, $n_s = 50$ and the simulation is run over 10 iterations where each iteration lasts 0.5 seconds. Additionally, the weighting parameters are selected as $q_u = 10^{-3}$, $q_{\delta u} = 10^{-2}$, $q_e = [1 \ 0]^T$, $q_x = 10^{-6} \cdot \mathbf{1}^{n_x}$, $q_{\delta x} = 3 \cdot 10^{-1} \cdot \mathbf{1}^{n_x}$, $s_x = 10^{-18} \cdot \mathbf{1}^{n_x}$ where $\mathbf{1}^a \in \mathbb{R}^a$ is a vector with all elements equal to 1. Note that in this selection of q_e , only the first element is non-zero. Hence, only the tracking error of the first state is penalized. The weighting parameters are chosen such that Conditions 1 and 3 are satisfied.

The state and input histories are shown in Figure 2 for the case when $n_i = 3$. Here, the input and states appear to have a transient phase before quickly settling to a steady state trajectory. Additionally, state x_1 is able to track the reference with small error. In fact, as shown in Figure 3, \mathbf{z}_j converges monotonically to \mathbf{z}_∞ as a function of j .

Interestingly, Figure 4 shows that the measured distances, as defined by the Euclidean norm, between \mathbf{z}_∞ as given by (38) and \mathbf{z}_{opt} as given in (52) are reduced monotonically as the length of the prediction horizon is increased. Hence, the RHILC approach allows for improved converged performance in comparison to traditional ILC techniques in which $n_i = 1$.

B. Simulation of Uncertain, Iteration-Varying System

To demonstrate the effectiveness of the RHILC scheme in a more realistic scenario, the control framework is applied to a simulated servo-positioning system with iteration-varying dynamics and embedded uncertainty.

For these simulations, the iteration-varying state disturbance signal, \mathbf{d}_j , is constructed as Gaussian noise centered at nominal value $\mathbf{d} = \mathbf{I}_{n_s} [1.2 \ 1.1]^T$. The plant dynamics are given by

$$\mathbf{x}_j = (\mathbf{G}^* + \Delta \mathbf{G}_j^*) \mathbf{u}_j + (\mathbf{F}^* + \Delta \mathbf{F}_j^*) \mathbf{x}_j^0 + \mathbf{d}_j \quad (62)$$

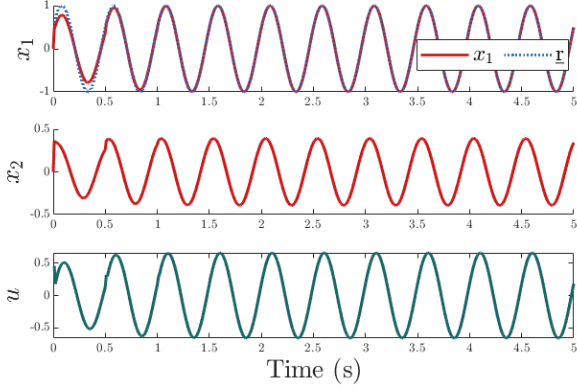


Figure 2: State and input sequence history over 10 continuous iterations where each iteration lasts 0.5 seconds with a prediction horizon length of $n_i = 3$.

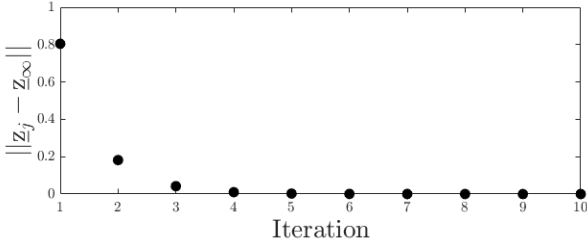


Figure 3: Convergence of z_j to z_∞ for $n_i = 3$.

where \underline{G}^* and \underline{F}^* are given by (4) and (5) with

$$\mathbf{A} = \begin{bmatrix} 0 & 1 \\ -0.35 & 0.87 \end{bmatrix}, \quad \mathbf{B} = \begin{bmatrix} 1.60 \\ 0.82 \end{bmatrix}. \quad (63)$$

Furthermore, $\Delta \underline{G}_j^*$ and $\Delta \underline{F}_j^*$ represent iteration-varying additive uncertainty that impacts the plant dynamics.

The learning matrices as given by (19) are based on the dynamic model

$$\underline{x}_j = (\underline{G} + \Delta \underline{G}_j) \underline{u}_j + (\underline{G} + \Delta \underline{G}_j) \underline{x}_j^0 \quad (64)$$

where \underline{G} and \underline{F} are constructed from (4) and (5) based on the nominal state space matrices in (61) and $\Delta \underline{G}_j$ and $\Delta \underline{F}_j$ are estimates of additive, time-varying changes to the nominal model.

The weighting parameters are updated from Section V-A with $q_{\delta x} = 3 \cdot 10^{-3} \cdot 1^{n_x}$ and $q_{\delta u} = 1 \cdot 10^{-3}$ such that Conditions 1 and 3 are satisfied. The simulation is run using $n_i = \{1, \dots, 6\}$ over 20 iterations.

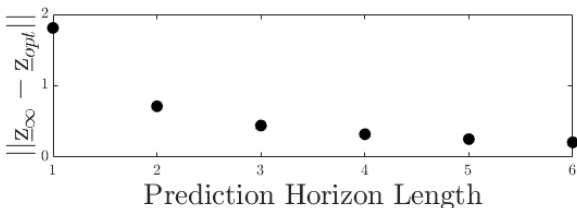


Figure 4: The distance between z_∞ and z_{opt} is reduced as the prediction horizon length increases.

The state and input sequence history is shown in Figure 5 for $n_i = 3$.

Additionally, the convergent behavior of the system is examined. Note that in this simulation, $\lim_{j \rightarrow \infty} (\underline{d}_j, \Delta \underline{G}_j^*, \Delta \underline{F}_j^*, \Delta \underline{G}_j, \Delta \underline{F}_j) = (\underline{d}, \mathbf{0}, \mathbf{0}, \mathbf{0}, \mathbf{0})$. In Figure 6, the evolution of z_j is depicted for various lengths of the prediction horizon. Note that while these signals tend to converge towards z_∞ , this evolution is non-monotonic due to the iteration-varying plant uncertainties and disturbances.

A comparison of z_∞ to z_{opt} as a function of the prediction horizon length is shown in Figure 7. Two key observations are made here. The first is that the use of a multi-iteration prediction horizon outperforms the single-iteration prediction horizon that would be used using standard ILC techniques. Additionally, note that a longer prediction horizon does not necessarily correspond to improved performance at convergence. Hence, an infinite horizon strategy for continuous ILC as proposed in [11] and [12] is not always the best choice when model uncertainties exist.

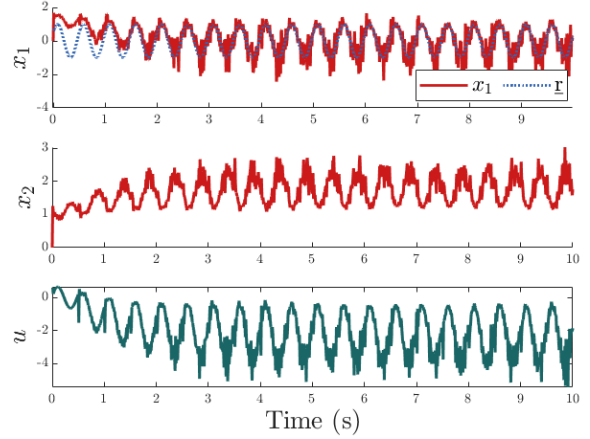


Figure 5: State and input sequences over 20 continuously operated iterations of the iteration-varying, uncertain system with a prediction horizon of $n_i = 3$.

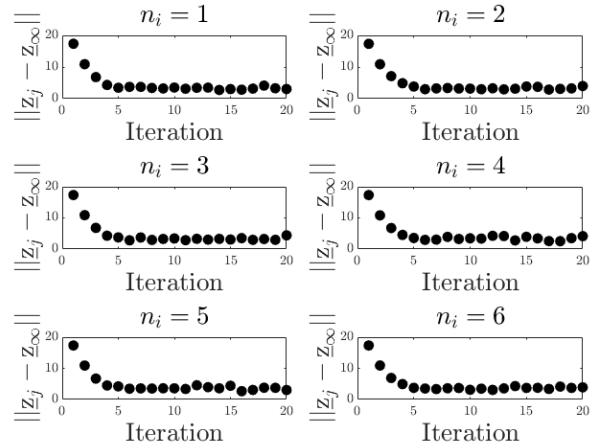


Figure 6: Convergence of z_j for different values of n_i .

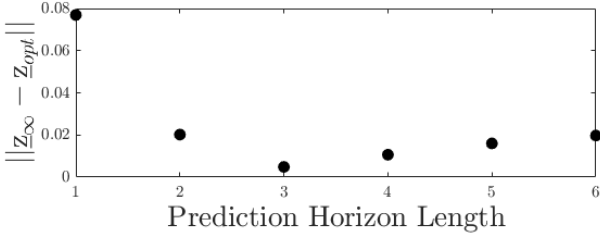


Figure 7: The distance between z_∞ and z_{opt} varies depending on the horizon length.

VI. CONCLUSIONS

This paper proposes an ILC strategy for continuously operated systems in which the initial condition is not reset between iterations. A multi-iteration dynamic model is defined using a lifted system representation that describes the behavior of the system in response to multi-iteration input sequences and arbitrary initial conditions. A closed form, receding horizon style update law for the input sequence is presented, with stability criteria and desired performance standards established for time-invariant and time-varying systems.

The scheme is then implemented through simulation on a servo-positioning system where it is observed that improved system behavior can be achieved by utilizing a multi-iteration receding horizon approach in comparison to traditional ILC strategies. Additionally, the improved converged performance of the system when utilizing a finite prediction horizon length is established when modelling inaccuracies and disturbances are present.

Future work includes extensions towards systems with general convex cost functions and for which full state information is not known, and the use of constrained optimal control strategies with terminal components to ensure improved closed-loop performance. Additional work will also address non-linear systems and systems with spatially-defined dynamics.

VII. APPENDIX

A. Performance Index Weighting Matrices

In (13), the weighting matrices Q_u , $Q_{\delta u}$, Q_e , Q_x , and $Q_{\delta x}$, are easily defined in terms of three functions,

- the “diagonal” matrix function, $f_D : \mathbb{R}^{n_a} \mapsto \mathbb{R}^{n_a \times n_a}$ which takes in an input vector, $v = [v_1, v_2, \dots, v_{n_a-1}, v_{n_a}]$, and outputs a matrix with the entries of the input vector along the diagonal and zeros elsewhere.

$$f_D(v) = \begin{bmatrix} v_1 & 0 & \dots & 0 & 0 \\ 0 & v_2 & \dots & 0 & 0 \\ \vdots & \vdots & \dots & \vdots & \vdots \\ 0 & 0 & \dots & v_{n_a-1} & 0 \\ 0 & 0 & \dots & 0 & v_{n_a-1} \end{bmatrix} \quad (65)$$

- the “repeated block diagonal” matrix function, $f_\Delta : (n_b, \mathbb{R}^{n_c \times n_d}) \mapsto \mathbb{R}^{n_b n_c \times n_b n_d}$ which accepts the positive integer, n_b , and an arbitrary matrix, $C \in \mathbb{R}^{n_c \times n_d}$, and

returns a block matrix with the input matrix repeated n_b times along the block diagonal

$$f_\Delta(n_b, C) \triangleq \begin{bmatrix} C & \mathbf{0} & \dots \\ \mathbf{0} & C & \dots \\ \vdots & \vdots & \ddots \end{bmatrix} \quad (66)$$

If we then define the vectors of user-selected scalar weights as

$$\begin{aligned} q_u &\triangleq [q_{u,1} \ \dots \ q_{u,n_u}]^T, \\ q_{\delta u} &\triangleq [q_{\delta u,1} \ \dots \ q_{\delta u,n_u}]^T, \\ q_e &\triangleq [q_{e,1} \ \dots \ q_{e,n_x}]^T, \\ q_x &\triangleq [q_{x,1} \ \dots \ q_{x,n_x}]^T, \\ q_{\delta x} &\triangleq [q_{\delta x,1} \ \dots \ q_{\delta x,n_x}]^T, \\ s_x &\triangleq [s_{x,1} \ \dots \ s_{x,n_x}]^T. \end{aligned} \quad (67)$$

Then the gain matrices Q_u , $Q_{\delta u}$, Q_e , $Q_{\delta e}$, Q_x that encode the relative importance of each term in the performance index are given by

$$\begin{aligned} Q_u &= f_\Delta(n_s, f_D(q_u)), \\ Q_{\delta u} &= f_\Delta(n_s, f_D(q_{\delta u})), \\ Q_e &= f_\Delta(n_s, f_D(q_e)), \\ Q_x &= f_\Delta(n_s, f_D(q_x)), \\ Q_{\delta x} &= f_\Delta(n_s, f_D(q_{\delta x})). \end{aligned} \quad (68)$$

B. Cost and Constraint Matrices for Compact Optimization Problem

In (51), the optimization problem is defined according to

$$\begin{aligned} \tilde{Q}_q &\triangleq \mathbf{E}_s^T \left(\mathbf{I}_u^T \hat{Q}_u \mathbf{I}_u - 2\mathbf{Q}_{\delta u} \right) \mathbf{E}_s + (\underline{\mathbf{G}}\mathbf{E}_s + \underline{\mathbf{F}}\mathbf{E}_e)^T \dots \\ &\quad \left(\mathbf{I}_x^T (\hat{Q}_x + \hat{Q}_e) \mathbf{I}_x - 2\mathbf{Q}_{\delta x} \right) (\underline{\mathbf{G}}\mathbf{E}_s + \underline{\mathbf{F}}\mathbf{E}_e) \\ \hat{q}_l &\triangleq (\underline{\mathbf{G}}\mathbf{E}_s + \underline{\mathbf{F}}\mathbf{E}_e)^T \left(\mathbf{I}_x^T (\hat{Q}_x + \hat{Q}_e) \mathbf{I}_x \underline{d} \dots \right. \\ &\quad \left. + \mathbf{I}_x^T (s_x - \hat{Q}_e \mathbf{I}_x \underline{r}) - 2\mathbf{Q}_{\delta x} \underline{d} \right) \\ \mathbf{W} &\triangleq \mathbf{E}_e - \mathbf{E}_F (\underline{\mathbf{G}}\mathbf{E}_s + \underline{\mathbf{F}}\mathbf{E}_e) \\ \mathbf{v} &\triangleq \mathbf{E}_F \underline{d} \end{aligned} \quad (69)$$

VIII. ACKNOWLEDGEMENTS

This work was funded by National Science Foundation grant numbers 1727371 and 1727779 entitled “Collaborative Research: An Economic Iterative Learning Control Framework with Application to Airborne Wind Energy Harvesting.”

REFERENCES

- [1] D. A. Bristow, M. Tharayil, and A. G. Alleyne, “A survey of iterative learning control,” *IEEE Control Systems Magazine*, vol. 26, no. 3, pp. 96–114, 2006.
- [2] Y. Wang, F. Gao, and F. J. Doyle, “Survey on iterative learning control, repetitive control, and run-to-run control,” *Journal of Process Control*, vol. 19, no. 10, pp. 1589 – 1600, 2009. [Online]. Available: <http://www.sciencedirect.com/science/article/pii/S0959152409001681>

- [3] S. Gunnarsson and M. Norrlöf, "On the design of ilc algorithms using optimization," *Automatica*, vol. 37, no. 12, pp. 2011–2016, 2001.
- [4] B. Chu, D. H. Owens, and C. T. Freeman, "Iterative learning control with predictive trial information: Convergence, robustness, and experimental verification," *IEEE Transactions on Control Systems Technology*, vol. 24, no. 3, pp. 1101–1108, 2016.
- [5] L. Wang and E. Rogers, "Predictive iterative learning control using laguerre functions," *IFAC Proceedings Volumes*, vol. 44, no. 1, pp. 5747 – 5752, 2011, 18th IFAC World Congress. [Online]. Available: <http://www.sciencedirect.com/science/article/pii/S1474667016445234>
- [6] N. Amann, D. H. Owens, and E. Rogers, "Predictive optimal iterative learning control," *International Journal of Control*, vol. 69, no. 2, pp. 203–226, 1998. [Online]. Available: <https://doi.org/10.1080/002071798222794>
- [7] M. Arif, T. Ishihara, and H. Inooka, "Prediction-based iterative learning control (pilc) for uncertain dynamic nonlinear systems using system identification technique," *Journal of Intelligent and Robotic Systems*, vol. 27, no. 3, pp. 291–304, Mar 2000. [Online]. Available: <https://doi.org/10.1023/A:1008162421594>
- [8] B. Chu, D. H. Owens, and C. T. Freeman, "Predictive gradient iterative learning control," in *2015 54th IEEE Conference on Decision and Control (CDC)*, 2015, pp. 2377–2382.
- [9] U. Rosolina, A. Carvalho, and F. Borrelli, "Autonomous racing using learning model predictive control," *Proceedings of the 2017 IFAC World Congress*, 2017, Toulouse, France.
- [10] M. Brunner, R. Ugo, J. Gonzales, and F. Borelli, "Repetitive learning model predictive control: An autonomous racing example," *Proceedings of the 56th Conference on Decision and Control*, 2017, Melbourne, Australia.
- [11] J. H. Lee, S. Natarajan, and K. S. Lee, "A model-based predictive control approach to repetitive control of continuous processes with periodic operations," *Journal of Process Control*, vol. 11, no. 2, pp. 195 – 207, 2001. [Online]. Available: <http://www.sciencedirect.com/science/article/pii/S0959152400000470>
- [12] M. Gupta and J. H. Lee, "Period-robust repetitive model predictive control," *Journal of Process Control*, vol. 16, no. 6, pp. 545 – 555, 2006. [Online]. Available: <http://www.sciencedirect.com/science/article/pii/S0959152406000035>
- [13] I. Lim and K. Barton, "Pareto optimization-based iterative learning control," *Proceedings of the American Control Conference*, 2013, Washington, D.C.
- [14] D. Clarke, C. Mohtadi, and P. Tuffs, "Generalized predictive control—part i. the basic algorithm," *Automatica*, vol. 23, no. 2, pp. 137 – 148, 1987. [Online]. Available: <http://www.sciencedirect.com/science/article/pii/0005109887900872>
- [15] D. A. Bristow, K. L. Barton, A. G. Alleyne, and W. S. Levine, "Iterative learning control," *The Control Systems Handbook: Control System Advanced Methods*, pp. 1–19, 2010.